Black Phosphorus

DOI: 10.1002/anie.201410108

Identifying the Crystalline Orientation of Black Phosphorus Using Angle-Resolved Polarized Raman Spectroscopy**

Juanxia Wu, Nannan Mao, Liming Xie, Hua Xu, and Jin Zhang**

Abstract: *An optical anisotropic nature of black phosphorus (BP) is revealed by angle-resolved polarized Raman spectroscopy (ARPRS), and for the first time, an all-optical method was realized to identify the crystal orientation of BP sheets, that is, the zigzag and armchair directions. We found that Raman intensities of A_g^1, B_{2g}, and A_g^2 modes of BP not only depend on the polarization angle α, but also relate to the sample rotation angle θ. Furthermore, their intensities reach the local maximum or minimum values when the crystalline orientation is along with the polarization direction of scattered light (e_s). Combining with the angle-resolved conductance, it is confirmed that A_g^2 mode intensity achieves a relative larger (or smaller) local maximum under parallel polarization configuration when armchair (or zigzag) direction is parallel to e_s. Therefore, ARPRS can be used as a rapid, precise, and nondestructive method to identify the crystalline orientation of BP layers.*

Black phosphorus (BP), the most stable allotrope of phosphorus, has become a new star in two-dimensional (2D) material family owing to its superior electrical and optical properties.[1] The BP field-effect transistors have shown attractive characteristics, including high room-temperature on/off ratio (ca. 10^5), well-developed current saturation, and exceptionally high carrier mobility up to 10000 $cm^2 V^{-1} s^{-1}$.[2] Furthermore, unlike other 2D materials (such as graphene and transition-metal dichalcogenides), BP has a direct bandgap for all thickness, tunable from 1.51 eV for monolayer to 0.31 eV for bulk.[1a,2,3] Most importantly, BP has the unique anisotropic nature, its optical,[4] electrical,[1a,5] thermoelectric,[6] mechanical[7] and other multitudinous properties are expected to show angle-dependence. In fact, recent works have revealed the high in-plane anisotropic conductivity of few-layer BP.[8] Moreover, theoretical calculations have predicted that these anisotropic behaviors can be effectively modulated by applying biaxial or uniaxial strain to the BP sample.[9] Therefore, the unique anisotropic nature of this intriguing material creates unprecedented possibilities for the realization of conceptually novel electronic, optoelectronic, and nano-mechanical devices which are not possible using other 2D materials.

However, most of these anisotropic properties of BP are still in theory, except the conductance and IR anisotropic nature.[1a,8] What is more, there is still a lack of an effective method to identify the crystalline orientation of BP, which is an essential precondition to the study of all above anisotropic properties. Although angle-resolved IR and conductance measurements have been used to identify the crystalline orientation of BP in previous report,[8] the relative complex process, rigorous instrument and limited angle resolution hinder their wide applications. Therefore, revealing the anisotropic properties of BP from experiment and developing a simple and precise method to identify its crystalline orientation seems to be of particular importance.

Herein, by revealing the optical anisotropic nature of BP using angle-resolved polarized Raman spectroscopy (ARPRS), we first successfully identify the crystal orientation of BP sheet using Raman spectroscopy, that is, the zigzag and armchair directions. The Raman intensity of A_g^1, B_{2g}, and A_g^2 modes in BP shows obvious periodic variation (90° or 180°) with the sample rotation angle under both parallel and cross-polarization configurations, and the variation features of these modes show great difference. All the results of the ARPRS are perfectly consistent with symmetry selection rules based on the Raman tensors, demonstrating the strong anisotropic nature of BP. Furthermore, according to the angle-resolved conductance and ARPRS, the zigzag and armchair directions of BP sheets can be identified from the intensity variation of A_g^2 mode as function of the sample rotation angle. Therefore, our results not only reveal an optical anisotropic nature of BP, but also supply a route for investigators that ARPRS can be used as a compass to precisely and nondestructively identify the crystalline orientation of BP, which is benefit to the further study on the anisotropic BP-based electronic, optoelectronic, and nano-mechanical devices.

[*] J. Wu,[+] N. Mao,[+] Prof. J. Zhang
Center for Nanochemistry, Beijing National Laboratory for Molecular Sciences, Key Laboratory for the Physics and Chemistry of Nanodevices, State Key Laboratory for Structural Chemistry of Unstable and Stable Species, College of Chemistry and Molecular Engineering, Peking University, Beijing, 100871 (P.R. China)
E-mail: jinzhang@pku.edu.cn
Prof. H. Xu
School of Materials Science and Engineering
Shaanxi Normal University, Xi'an, 710062 (P.R. China)
E-mail: xuhua-nano@snnu.edu.cn
Prof. L. Xie
CAS Key Laboratory of Standardization and Measurement for Nanotechnology of Chinese Academy of Sciences, National Center for Nanoscience and Technology, Beijing, 100190 (P.R. China)
J. Wu[+]
Academy for Advanced Interdisciplinary Studies
Peking University, Beijing, 100871 (P.R. China)
[+] These authors contributed equally to this work.

[**] This work was supported by the NSFC (21233001, 21129001, 51272006, 51121091, and 51432002), MOST (2011YQ0301240201 and 2011CB932601), and the China Postdoctoral Science Foundation (2013M530468).
Supporting information for this article is available on the WWW under http://dx.doi.org/10.1002/anie.201410108.

Similar to graphite, BP atomic layers are stacked together with van der Waals interaction while the single layer is covalently bonded by sp^3 phosphorus atoms. Owing to the sp^3 hybridization, each phosphorus atom is covalently bonded to three neighboring phosphorus atoms and has one lone pair electrons, thus forming a structure of quadrangular pyramid as shown in Figure 1 a. This hybridization structure, in turn,

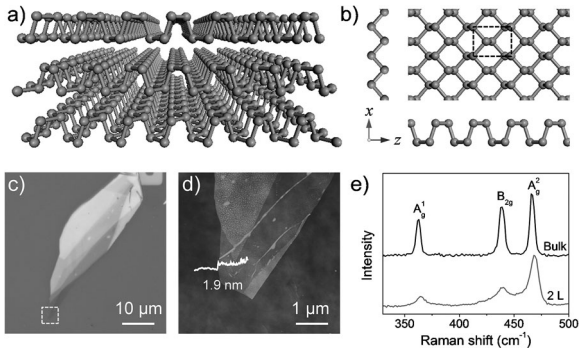

Figure 1. a) The puckered structure of a few-layer BP sheet. b) Top view of monolayer BP. The *x* and *z* axis are along zigzag and armchair directions, respectively. c) OM and d) AFM images of a few-layer BP sheet. e) Raman spectra of bilayer and bulk BP.

determines the puckered honeycomb structure of BP, which has reduced symmetry compared to graphite, resulting in its unique in-plane anisotropic properties. Figure 1 b shows the top view of monolayer BP sheet. Four phosphorus atoms constituted a unit cell of BP, which is indicated in the dashed rectangle. In the Raman tensor coordinate system, the *x* and *z* axis are in the zigzag and armchair direction, respectively.

Typical OM and AFM images of few-layer BP are shown in Figure 1 c,d. Considering a layer-to-layer spacing of 0.53 nm, we identified the few-layer BP with thickness down to around 1.9 nm, corresponding to two atomic layers of BP. The measurement height from AFM image is larger than the theoretical value (ca. 1.1 nm), which could be due to the instrumental offset (ca. 0.5 nm) and the adsorbates between the sample and substrate. However, few-micrometer scale thin BP flakes are usually too small for Raman and electrical experiments. In this work, we performed Raman and electrical measurements on BP layers with a thickness varying from 3 to 10 nanometers (5 to 20 layers). The Raman spectra of bilayer and bulk BP are shown in Figure 1 e. Three typical Raman peaks, one out-of-plane mode (A_g^1, ca. 363 cm^{-1}) and two in-plane modes (ca. 440 cm^{-1} for B_{2g} and ca. 467 cm^{-1} for A_g^2), are observed in both bilayer and bulk BP. Compared to the bilayer BP, A_g^2 mode shifts to lower frequency in bulk material, which is consistent with the previous report.[10]

Bulk BP belongs to D_{2h} space group, and there are 12 lattice vibrational modes at the Γ point.[11] Six of them are Raman-active modes (Figure 2 a), while only A_g^1, B_{2g}, and A_g^2 modes can be detected when the incident laser is perpendicular to the sample plane (as indicated in Figure 1 e) according to the symmetry selection rule. As shown in Figure 2 b, *x* and *z* are the crystal orientation, and e_i and e_s are the polarization

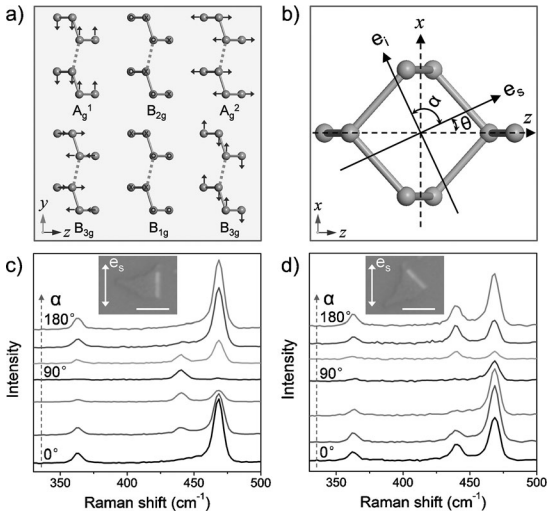

Figure 2. a) Atomic displacements for Raman-active modes in BP. b) The configuration in the polarized Raman experiments. c),d) Raman spectra of BP sample with different polarization angle α. Insets in (c) and (d) are the OM images, and the scale bar is 5 μm.

vectors of incident laser and scattered light, respectively. So, α is the polarization angle between e_i and e_s, and θ is the sample rotation angle between *z* (armchair) and e_s. Figure 2 c shows the polarized Raman spectra of a BP sheet with different polarization angle α, which were collected with the sample direction as the OM image shown in the inset. It can be seen that the relative intensities of these three modes change significantly with polarization angle α. A_g^1 and A_g^2 modes can be detected under parallel polarization configuration ($\alpha = 0°/180°$), while the B_{2g} mode is forbidden. The intensity of the B_{2g} mode increases and two A_g modes become weaker as α gradually approaches 90°. Only the B_{2g} Raman mode can be observed, while A_g modes are forbidden under the cross-polarization configuration ($\alpha = 90°$). More interesting is that different phenomenon can be observed if the BP sample was rotated, such as it was rotated 45° anticlockwise (Figure 2 d). All these three Raman modes can be detected under parallel polarization configuration ($\alpha = 0°/180°$), while they become much weaker and B_{2g} mode disappears when α approaches 90°. The above experimental results indicate that the intensity of Raman modes in BP not only depends on the polarization angle α, but also relates to the sample rotation angle θ, which demonstrates the optical anisotropy of BP. At the same time, the results also remind us that the crystalline orientation should be considered if we want to study the thickness-dependent Raman spectra of BP in future. In this regard, it is critical to find an effective method to identify the crystalline orientation of BP.

Owing to the fact that the crystalline orientation is unknown when the polarized Raman measurements were carried out, it is of interest to consider the generalized form of the Raman tensors for BP with a sample rotation angle θ. The generalized form of Raman tensors (the detailed transformation process is shown in section 1 in Supporting Information) can be expressed as follows:[12]

$$\tilde{R}'(A_g) = \begin{pmatrix} a\cos^2\theta + c\sin^2\theta & 0 & \frac{1}{2}(a-c)\sin 2\theta \\ 0 & b & 0 \\ \frac{1}{2}(a-c)\sin 2\theta & 0 & a\sin^2\theta + c\cos^2\theta \end{pmatrix}$$
$$\tilde{R}'(B_{2g}) = \begin{pmatrix} -e\sin 2\theta & 0 & e\cos 2\theta \\ 0 & 0 & 0 \\ e\cos 2\theta & 0 & e\sin 2\theta \end{pmatrix} \quad (1)$$

The intensity of a given Raman mode, which is related to the Raman tensor and scattering geometry, is proportional to the expression $|e_i \cdot \tilde{R} \cdot e_s|^2$.[13] According to the generalized form of Raman tensors, the intensity of A_g and B_{2g} Raman modes are closely related to the sample rotation angle θ under both parallel and cross-polarization configurations, which reach the local maxima or minima when e_s along the crystalline orientation (see Section S1 in the Supporting Information). To reveal this relationship, we measured the Raman spectra of BP sheet under both parallel and cross-polarization configurations as the sample rotated from 0° to 360° (for experimental details and the spectra, see the Supporting Information, Section S2). The polar plots of the fitted peak intensities of these Raman modes as function of sample rotation angle θ are shown in Figure 3. It can be clearly seen that different Raman modes show different periodic variation features. Under parallel polarization configuration, the A_g^1 mode intensity has a 180° variation period, which is almost undetectable for $\theta = 0°/180°$, while its intensity achieves the maximum for $\theta = 90°$. The A_g^2 mode has a 90° variation period, which reaches the local maximum at $\theta = 0°/90°$, and becomes much weaker at $\theta = 45°$. It should be noted that there are two different local maxima for the A_g^2 mode, which is attributed to the different values of a and c in the Raman tensor. Furthermore, the intensity of the B_{2g} mode is proportional to $\sin^2 2\theta$ with 90° variation period, which achieves maximum at $\theta = 45°$ and is completely forbidden at $\theta = 0°/90°$. The case is different under the cross-polarization configuration; the intensities of all these three Raman modes exhibit 90° variation period with the sample rotation angle θ. A_g^1 and A_g^2 modes ($I \propto \sin^2 2\theta$) are forbidden at $\theta = 0°/90°$, and they have the local maxima at $\theta = 45°$, while the B_{2g} mode ($I \propto \cos^2 2\theta$) achieves a local maximum at $\theta = 0°/90°$ and is forbidden at $\theta = 45°$. From above results we can see that with the crystalline orientation (zigzag or armchair direction) along the polarization direction of the scattered light, the intensity of these Raman modes reaches a local maximum or minimum value, which is very consistent with the scattering efficiency calculated from the Raman tensors. These results further demonstrate the optical anisotropic nature of BP, and most importantly, it can be used to identify the crystalline orientation of BP sheets.

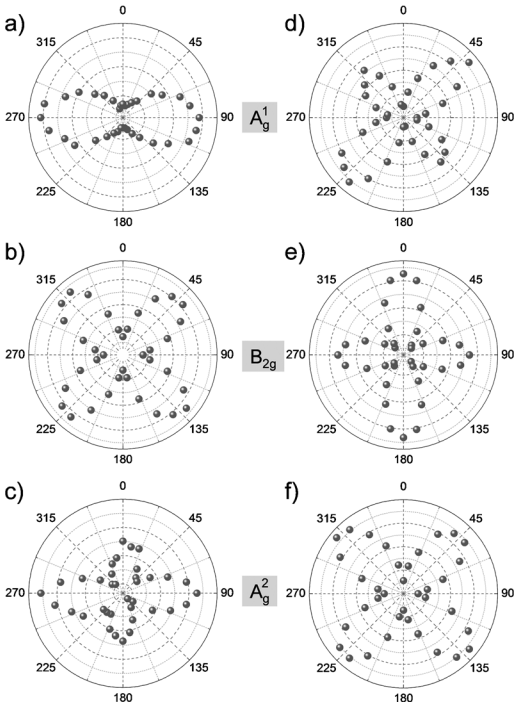

Figure 3. Polar plots of the fitted peak intensities of (a, d) A_g^1, (b, e) B_{2g}, and (c, f) A_g^2 modes as a function of sample rotation angle θ under (a–c) parallel and (d–f) cross-polarization configurations.

According to the intensity variation period of the A_g^2 mode under parallel polarization configuration, we can identify the armchair or zigzag direction, but we cannot ascertain the specific direction of the crystalline orientation of BP. Recently, theoretical and experimental results show that the hole conductance of BP along armchair direction will be larger than that along zigzag direction. To further confirm the z (armchair) and the x (zigzag) directions of the BP sheet, we measured the angle-resolved conductance of BP sheet similar to the method reported previously.[8] Briefly, 12 electrodes (5 nm Cr/60 nm Au) were fabricated on the BP sheet spaced at an angle of 30° along the directions as shown in Figure 4a. Here, we define the Y axis as the 0° reference, which is also the direction of polarization vector of scattered light (e_s). We performed the conductance measurements by applying an electric field (3 V) across each pair of diagonally positioned electrodes separated by 12 μm at 180° apart, and the results

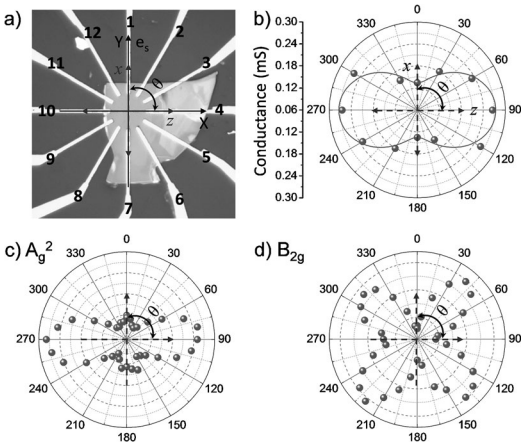

Figure 4. a) Optical image of the few-layer BP device with 12 electrodes spaced at 30° apart. b) Polar plots of the conductance as a function of angle β measured with 3 V electric field along the 12 directions on the BP sheet. c),d) Polar plots of the fitted peak intensity of (c) A_g^2 and (d) B_{2g} modes as a function of rotation angle θ under parallel polarization configuration.

are plotted in Figure 4b in polar coordinates. The anisotropic conductivity of BP can be fitted with the following equation $\sigma_\beta = \sigma_x \cos^2(\beta-\phi) + \sigma_z \sin^2(\beta-\phi)$,[8] where σ_x and σ_z refer to the conductance of BP along x and z directions, respectively; β is the angle with respect to the 0° reference, along which the electric field is applied to measure the conductance; σ_β is the conductance along β direction; ϕ is the angle between x direction and 0° reference. The fitting results are as follows: $\sigma_x = 0.13$ mS, $\sigma_z = 0.27$ mS, $\phi = -0.04°$, which means that the zigzag direction is coincident with the 0° reference, the ratio σ_z/σ_x is around 2.1, near to the value previously reported.[8]

Now, we come to study the corresponding angle-resolved polarized Raman of this sample. Similar to the above experiment, Raman signals were collected with the sample rotated anticlockwise from the sample direction in Figure 4a under parallel polarization configuration. Figure 4c shows the polar plots of the peak intensity of A_g^2 mode as a function of rotation angle θ. The A_g^2 mode reaches a relative smaller local maximum intensity at $\theta = 0°$, where the x direction (zigzag direction) is along with the 0° reference. When we rotate the sample 90° anticlockwise, where the z direction (armchair direction) is parallel to the 0° reference, a relatively larger local maximum intensity can be obtained. Therefore, the relative smaller local maximum and larger local maximum intensities of A_g^2 mode correspond to the zigzag and armchair directions of BP, respectively. Of course, not all these three Raman modes can be used to identify the specific crystalline orientation, such as the B_{2g} mode (Figure 4d), the two adjacent local minimum intensities should be corresponding to the zigzag and armchair directions, however, the same local maximum intensities make it incapable to distinguish them. In a word, we can directly identify the specific zigzag and armchair directions of BP sheets from ARPRS in the future. Compared to the angle-resolved conductance which is limited to the smaller angle resolution and the fugitive contact resistance of each pair of electrodes, ARPRS can more precisely and conveniently identify the crystalline orientation of BP sheets. In particular, this approach can nondestructively identify the crystalline orientation of BP sheets with any irregular morphology (Supporting Information, Section S3), which is of benefit to the future study on the anisotropic properties of BP sheets.

In summary, we revealed a novel optical anisotropic nature of BP using ARPRS, which was developed as a rapid, precise, and nondestructive method to identify the specific zigzag and armchair crystalline direction of BP sheets. For an arbitrarily located sample, by rotating it under parallel polarization configuration, the A_g^2 band intensity achieves the larger (or smaller) local maximum when the armchair (or zigzag) direction is along the polarization direction of scattered light. This simple and precise crystalline orientation identification method is benefit to the future study of the anisotropic nature of BP. Furthermore, this method can be expanded to other 2D materials with anisotropic nature, and the great success of the ARPRS in the study of the anisotropic materials like BP provides great help for further revealing the anisotropic manner of electrons, phonons, and their interactions with photons within the plane of the layers of BP film.

Experimental Section

Few-layer BP samples were first exfoliated using the standard mechanical cleavage method from bulk BP crystal (from smart-elements) and then deposited on SiO_2/Si (300 nm thick oxide) substrate. The morphology and the thickness of few-layer BP sheets were characterized by optical microscopy (OM) and atomic force microscopy (AFM). Raman spectra were collected on a JY Horiba HR800 Raman system with 514.5 nm (2.41 eV) line from an Ar^+ laser. The laser power on the sample was kept below 100 μW to avoid destroying the sample. A 100× objective and 600 lines/mm grating (spectral resolution was about 1 cm^{-1}) were used to collect Raman signals. For polarization-dependent Raman experiments, a polarization analyzer was placed between edge filter and detector to obtain the parallel polarization configuration, the cross-polarization condition was achieved by placing a half-wave plate in the incident laser path, and polarized Raman spectra with different angles α were obtained by rotating the half-wave plate with angle $\alpha/2$ from parallel polarization configuration. Electrical contacts with BP sample were achieved using standard electron beam lithography and thermal evaporation of 5 nm Cr and 60 nm Au.

Received: October 15, 2014
Revised: December 13, 2014
Published online: January 21, 2015

Keywords: anisotropy · black phosphorus · crystalline orientation · phosphorene · polarized Raman spectroscopy

[1] a) H. Liu, A. T. Neal, Z. Zhu, Z. Luo, X. F. Xu, D. Tomanek, P. D. D. Ye, *ACS Nano* **2014**, *8*, 4033 – 4041; b) L. K. Li, Y. J. Yu, G. J. Ye, Q. Q. Ge, X. D. Ou, H. Wu, D. L. Feng, X. H. Chen, Y. B. Zhang, *Nat. Nanotechnol.* **2014**, *9*, 372 – 377; c) H. Liu, A. T. Neal, M. W. Si, Y. C. Du, P. D. Ye, *IEEE Electron Device Lett.* **2014**, *35*, 795 – 797.

[2] J. S. Qiao, X. H. Kong, Z. X. Hu, F. Yang, W. Ji, *Nat. Commun.* **2014**, *5*, 4475.

[3] M. Buscema, D. J. Groenendijk, S. I. Blanter, G. A. Steele, H. S. J. van der Zant, A. Castellanos-Gomez, *Nano Lett.* **2014**, *14*, 3347 – 3352.

[4] A. Morita, *Appl. Phys. A* **1986**, *39*, 227 – 242.

[5] S. Zhang, J. Yang, R. J. Xu, F. Wang, W. F. Li, M. Ghufran, Y.-W. Zhang, Z. F. Yu, G. Zhang, Q. H. Qin, et al., *ACS Nano* **2014**, *8*, 9590 – 9596.

[6] J. Zhang, H. J. Liu, L. Cheng, J. Wei, J. H. Liang, D. D. Fan, J. Shi, X. F. Tang, Q. J. Zhang, **2014**, arXiv:1405.3348.

[7] H. O. H. Churchill, P. Jarillo-Herrero, *Nat. Nanotechnol.* **2014**, *9*, 330 – 331.

[8] F. N. Xia, H. Wang, Y. C. Jia, *Nat. Commun.* **2014**, *5*, 4458.

[9] a) G. Z. Qin, Q.-B. Yan, Z. Z. Qin, S. Y. Yue, H. J. Cui, Q. R. Zheng, G. Su, *Sci. Rep.* **2014**, *4*, 6946; b) R. X. Fei, L. Yang, *Nano Lett.* **2014**, *14*, 2884 – 2889; c) H. Y. Lv, W. J. Lu, D. F. Shao, Y. P. Sun, *Phys. Rev. B* **2014**, *90*, 085433; d) R. X. Fei, L. Yang, *Appl. Phys. Lett.* **2014**, *105*, 083120.

[10] W. L. Lu, H. Y. Nan, J. H. Hong, Y. M. Chen, C. Zhu, Z. Liang, X. Y. Ma, Z. H. Ni, C. H. Jin, Z. Zhang, *Nano Res.* **2014**, *7*, 853 – 859.

[11] a) J. Ribeiro-Soares, R. M. Almeida, L. G. Cancado, M. S. Dresselhaus, A. Jorio, **2014**, arXiv:1408.6641; b) S. Sugai, T. Ueda, K. Murase, *J. Phys. Soc. Jpn.* **1981**, *50*, 3356 – 3361; c) S. Sugai, I. Shirotani, *Solid State Commun.* **1985**, *53*, 753 – 755.

[12] J. B. Bates, A. S. Quist, *J. Chem. Phys.* **1972**, *56*, 1528 – 1533.

[13] Y. Y. Zhao, X. Luo, H. Li, J. Zhang, P. T. Araujo, C. K. Gan, J. Wu, H. Zhang, S. Y. Quek, M. S. Dresselhaus, et al., *Nano Lett.* **2013**, *13*, 1007 – 1015.

